Spatioselective Growth of Metal-Organic Framework Nanocrystals on Compositionally Anisotropic Polymer Particles

*Tae-Hong Park, Kyung Jin Lee, Sangyeul Hwang, Jaewon Yoon, Christof Woell, and Joerg Lahann**

Spatio-selective crystal growth of a metal-organic framework (MOF) material is demonstrated on partially carboxylic acid-functionalized cross-linked Janus particles. The anisotropic seed particles have been prepared by electrohydrodynamic co-jetting followed by shape-shifting and subsequent chemical modifications of the Janus particles. This work combines critical advances in the synthesis and processing of rationally designed polymers, advanced microparticle preparation of bicompartmental, well-shaped seed particles, and a novel MOF growth procedure to demonstrate, for the first time, the spatio-selective growth of MOF nanocrystals on anisotropic polymer microparticles.

Metal-organic frameworks (MOFs) featuring well-defined pores and excessive porosity may find a pivotal role in a wide range of future applications ranging from catalysis,[1] separation,[2] to drug delivery.[3] Moreover, the ability to design well-organized MOF arrays on micropatterned substrates may enable further progress in fields of membranes for filtration and gas separation, catalytically active coatings, and therapeutic delivery systems.[4] A particular focus of recent MOF activities has targeted the spatio-selective growth of MOF crystals on two-dimensional substrates; for example, lithography and printing techniques resulted in well-defined two-dimensional MOF-patterned films.[5]

T.-H. Park,[+] K. J. Lee,[++] S. Hwang, J. Lahann
Department of Chemical Engineering
University of Michigan
Ann Arbor, MI 48109, USA
E-mail: lahann@umich.edu
J. Yoon, J. Lahann
Macromolecular Science and Engineering
University of Michigan
Ann Arbor, MI 48109, USA
C. Woell, J. Lahann
Institute for Functional Interfaces
Karlsruhe Institute of Technology
76344 Eggenstein-Leopoldshafen, Germany
J. Lahann
Biointerfaces Institute
University of Michigan
Ann Arbor, MI 48109, USA
[+]Present address: Nuclear Chemistry Research Division, Korea Atomic Energy Research Institute, Daejeon 305–353, Korea
[++]Present address: Department of Fine Chemical Engineering and Applied Chemistry, College of Engineering, Chungnam National University, Daejeon 305–764, Korea

DOI: 10.1002/adma.201305461

While there is a growing body of methods for the site-specific modification of two-dimensional systems and isotropic decoration of three-dimensional microstructures, such as particles, with MOFs,[4,6] little is known for the spatio-selective growth of porous coordination polymers on 3D objects, This creates an immanent need for generally applicable strategies of the spatio-selective growth of MOF crystals on particulate objects, which likely develop unprecedented catalysts, adsorbents, or delivery carriers. One critical prerequisite of building such novel 3D microstructures will be the design of appropriate anisotropic seed structures, i.e., patchy microparticles. A range of different patchy particles displaying two or more distinct surface patterns, or shapes have been explored[7] including particles to be used as catalysts,[8] microactuators,[9] smart drug vehicles,[10] or switchable displays.[11] These compositionally anisotropic particles have been fabricated via diverse synthetic strategies including microfluidic processing, block copolymer self-assembly, particle replication in non-wetting templates (PRINT); to name just a few examples.[12] Alternatively, electrohydrodynamic co-jetting has successfully been used to prepare compartmentalized particles and fibers.[13] Multicompartmental particles can be prepared through laminar co-flow of several compositionally dissimilar polymer solutions, which may contain a broad range of additives, such as functionalized polymers, dyes, and inorganic materials in the respective fluid flows.[14] If appropriately designed polymers with different reactive chemical groups are selectively embedded in compartments, the resulting particles can then be further altered through spatially controlled surface modification. Through this two step approach, substantially more complex properties and previously unrealized sets of functions can be achieved.[15]

Herein, we report the engineering of a new type of hierarchically functionalized colloidal composite particles, where MOF nanocrystals are spatio-selectively grown on the surface of compositionally anisotropic microparticles. The patchy seed particles are initially prepared via electrohydrodynamic co-jetting of two distinct polymer solutions with differently functionalized polymers. Additionally, the inclusion of paramagnetic nanoparticles into one compartment can provide porous, magnetically controllable anisotropic colloids that may hold potential for switchable catalysts or traceable delivery vehicles.

Inspired by the spatio-selective patterning of MOF crystals on micropatterned, carboxylic acid functionalized 2D substrates,[4a,16] we pursued patchy particles featuring one hemisphere with carboxylic acid groups for the spatio-selective growth of MOF materials. The initial seed particles were

ADVANCED MATERIALS
www.advmat.de

www.MaterialsViews.com

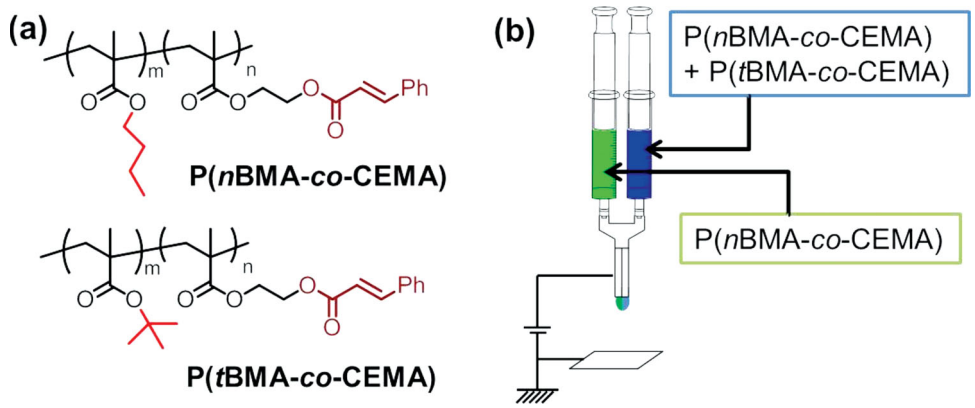

Scheme 1. (a) Chemical structure of poly(*n*-butyl methacrylate-*co*-cinnamoylethyl methacrylate) and poly (*t*-butyl methacrylate-*co*-cinnamoylethyl methacrylate) (b) Illustration of the electrohydrodynamic co-jetting process used to create patchy seed particles.

prepared by electrohydrodynamic co-jetting. The delicate interplay between solvent and polymers selected for the two compartments is an important parameter for successful electrohydrodynamic co-jetting.[14] Process-related factors often govern the selection of appropriate chemistries for subsequent chemical modification steps. Selective surface modification of different surface patches typically requires polymers with substantially different composition and functional side groups, yet electrohydrodynamic co-jetting often favors the use of quiet similar polymers in both compartments. In this work, we identified two different photocrosslinkable functional copolymers with different ester side groups: poly(*n*-butyl methacrylate-*co*-cinnamoylethyl methacrylate), P(*n*BMA-*co*-CEMA) and poly(*t*-butyl methacrylate-*co*-cinnamoylethyl methacrylate), P(*t*BMA-*co*-CEMA) (**Scheme 1**a). The Cu-catalyzed atom transfer radical polymerization (ATRP) reactions of butyl methacrylate and cinnamoylethyl methacrylate yielded both co-polymers in good yields (Supporting Information). The polymers contained cinnamolyethyl groups (10 mol%), which are photocrosslinkable via [2+2]cyclization reactions of vinyl groups,[17] whereas *n*- or *t*-butyl methacrylate moieties were selected to independently tailor the overall polymer property as well as the surface reactivity after electrohydrodynamic co-jetting.

Patchy polymethacrylate microparticles were prepared by electrohydrodynamic co-jetting of two sets of polymer solutions generated by laminar flow from a side-by-side arrangement of capillary jetting needles (Scheme 1b, Supporting Information). Although several attempt with different polymer compositions were unsuccessful to obtain compartmentalized particles, a very stable biphasic Taylor cone was obtained when P(*n*BMA-*co*-CEMA) in one solution was co-jetted with a mixture of P(*n*BMA-*co*-CEMA) and P(*t*BMA-*co*-CEMA) (3.5:1) as the second jetting solution. **Figure 1** displays the scanning electron microscopy (SEM) and confocal laser scanning microscopy (CLSM) images of the resulting microparticles, indicating irregular shapes and even dimples in some particles. The compositionally different compartments are likely solidified with dissimilar solvent evaporation rates during the atomization of charged jets, leading to these uneven and non-spherical particles.[18] Nevertheless, the biphasic Taylor cone was extremely stable for several hours and gave rise to a well-defined interface between the two compartments. Moreover, the bicompartmental character of the particles is unambiguously demonstrated by localized areas of different fluorescent polymers. A trace amount of these fluorescent dyes was added to the two different jetting solutions to distinguish the different compartments using confocal laser scanning microscopy after electrohydrodynamic co-jetting. The bicompartmental characteristic of these microparticles, thus, indicates that P*t*BMA moieties are localized in one compartment and composes ~20% of the respective hemisphere, whereas P(*n*BMA-*co*-CEMA) accounts for the reminder as well as the opposite compartment.

While the bicompartmental architecture of the particles was very encouraging, the uneven shape was less ideal. While we recognize that inherently nonspherical polymer particles have shown unique properties and are desirable for certain

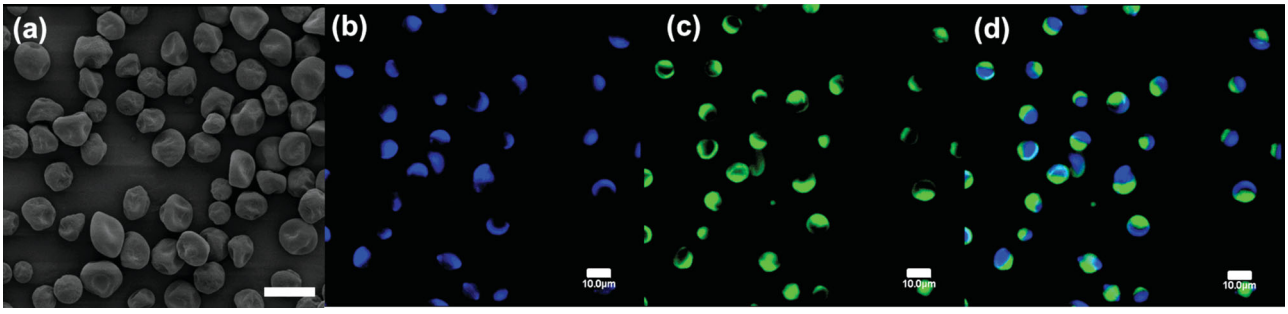

Figure 1. (a) SEM and (b-d) CLSM images of patchy particles, as jetted (scale bar: 10 µm). Images (b) and (c) were obtained by confocal laser scanning microscopy from the blue and green channels, respectively, and are shown along with the corresponding overlay image (d).

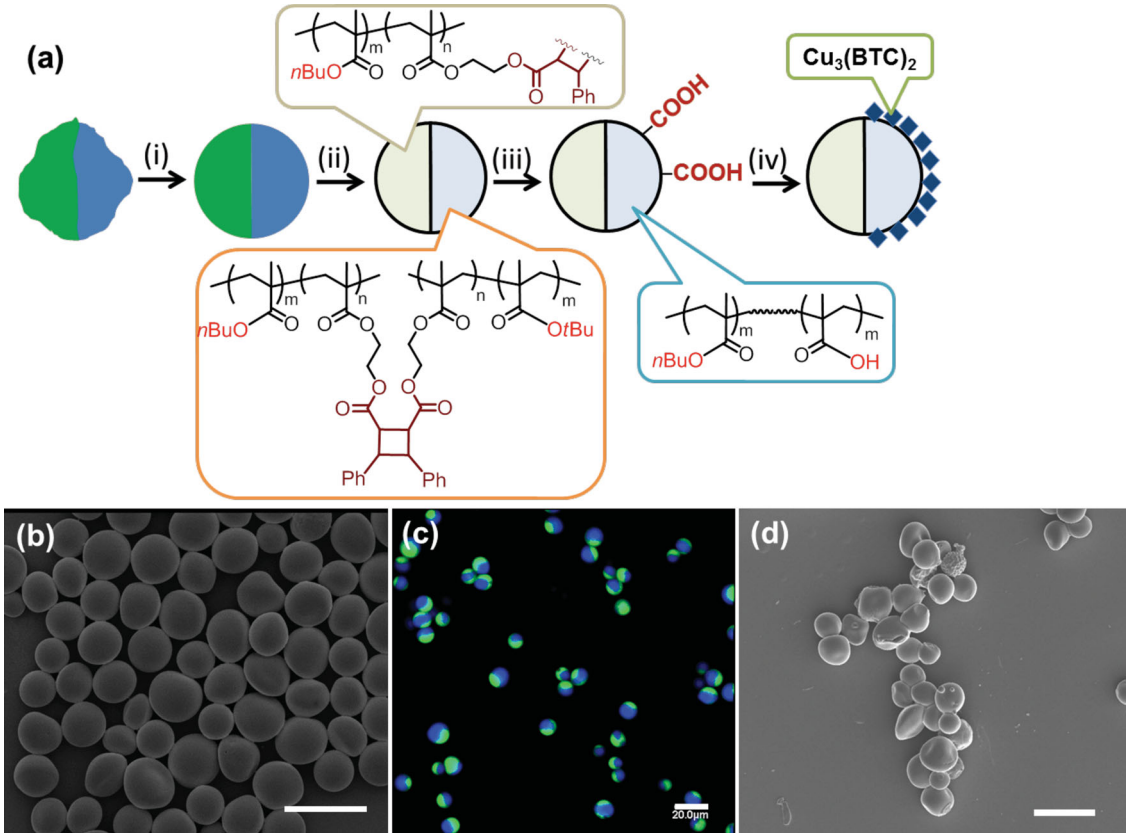

Figure 2. (a) Scheme of seed particle shape evolution and spatio-selctive $Cu_3(BTC)_2$ MOF nanocrystal growth on patchy seed particles; (i) sonication, 2 min; (ii) photocrosslinking, 300 nm, 2 h; (iii) deprotection, TFA, CH_2Cl_2, 2 h; (iv) layer-by-layer like crystallization of $Cu_3(BTC)_2$ using $Cu(OAc)_2$ and trimesic acid (H_3BTC). (b) SEM and (c) overlay CLSM images after sonication for 2 min. (d) SEM image after consecutive photocrosslinking and deprotection reactions. Scale bar: 20 µm.

applications,[19] the irregular shape of the particles in Figure 1 could be of concern, as it may lead to difficulty in precise particle engineering during the following step: the spatioselective MOF growth on the surface of bicompartmental microparticles. Therefore, we evaluated a recently developed methodology for shape shifting of polymer particles, which was used in the past to convert microcylinders into spheres.[9] Induced by short ultrasonication, non-spherical microparticles were found to minimize their free surface energy – taking on perfectly spherical shapes. The shape reconfiguration happens at temperatures above the glass temperature (T_g) of the polymer used to prepare the particle compartment.[9] We employed differential scanning calorimetery (DSC) measurements to determine the T_g of P(*n*BMA-*co*-CEMA) and P(*t*BMA-*co*-CEMA) to be 27.1 °C and 114.3 °C, respectively. Because the T_g of P(*t*BMA-*co*-CEMA) is substantially higher, we chose the polymer with the lower T_g [P(*n*BMA-*co*-CEMA)] as the main component of both compartments. The SEM and CLSM images of particles after ultrasonication for various time points between 0 and 10 min are displayed in Figure S4. After sonication for 2 min, the shape of irregularly dimpled bicompartmental particles became spherical (**Figure 2**b and S4). This is in stark contrast to the initial bicompartmental microparticles as-jetted, which are shown in Figure 1a. Importantly, CLSM confirmed the presence of two distinct compartments after shape-shifting into spheres (Figure 2c and S4) by localized dye fluorescence, indicating that the anisotropic composition of the particles was preserved after sonication for up to 3 min. In conclusion, ultrasonication for 2 min was found to be optimum for the irregular bicompartmental particles to be converted into near-to-perfect spheres, while minimizing polymer diffusion.

Thereafter, well-defined spherical particles were crosslinked via the photoreaction of cinnamoyl groups under UV light (λ = 300 nm),[17] which locks in their spherical shape and enables the particles to suspend in an organic solvent without any form of deformation (Figure 2d) The IR spectra confirmed the reaction within the compartments (**Figure 3**). While the jetted particles exhibit the combination of both polymer IR spectra, UV irradiation led to substantial decrease in the double bond peak at 1639 cm^{-1} (Figure 3c and d) indicating the sufficient [2+2]cyclization of cinnamoyl groups and crosslinking. The subsequent deprotection of *t*BMA groups with trifluoroacetic acid (TFA) in CH_2Cl_2 for 2 hr selectively diminished the signals at 1383 and 1363 cm^{-1}, and at 839 cm^{-1} that are attributed to the C-H bending and -CH_3 rocking of the *t*-butyl group of P(*t*BMA-*co*-CEMA), respectively (Figure 3c and e). Such spectral change unambiguously indicates that the deprotection of *t*-butyl ester was successful and accordingly provided patchy microparticles that were functionalized with carboxylic acid at one hemisphere only (Figure 2a).

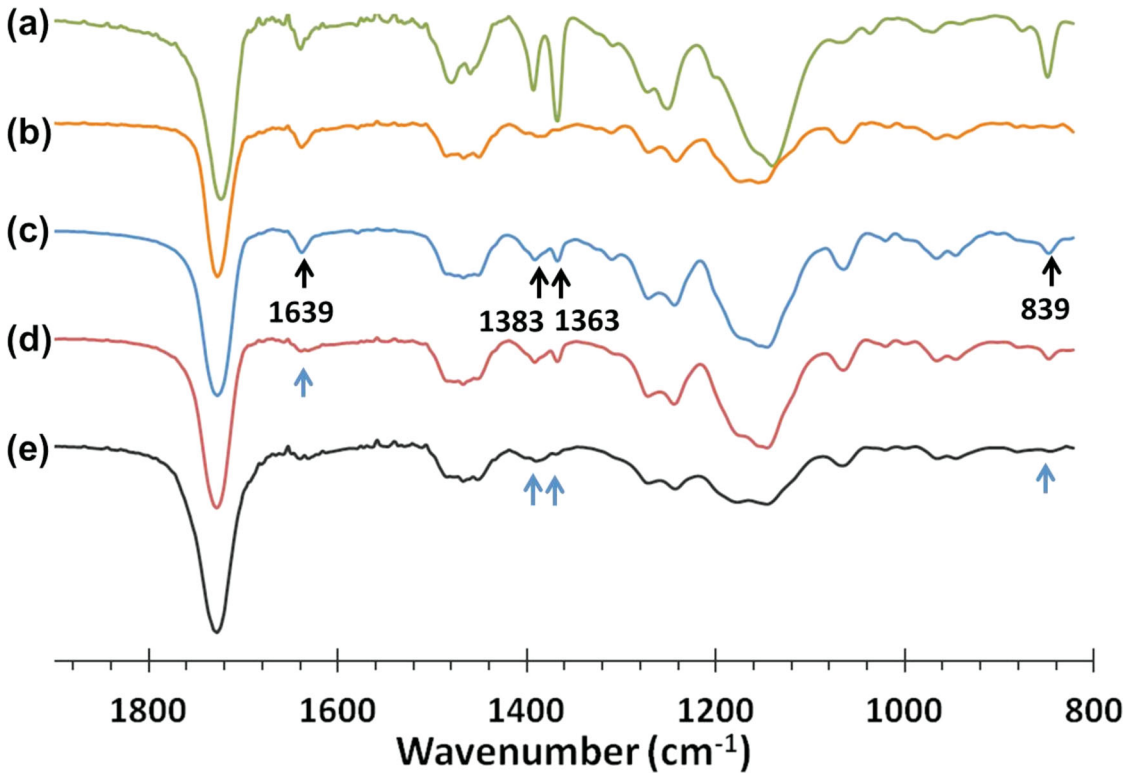

Figure 3. IR spectra of (a) P(*t*BMA-*co*-CEMA) and (b) P(*n*BMA-*co*-CEMA), and bicompartmental particles (c) as jetted, (d) after photocrosslinking, and (e) after deprotection.

Finally, with anisotropic and well-shaped seed particles in hand, we attempted the selective growth of MOF crystals on the surface of one hemisphere of the patchy particles. We chose a highly porous $Cu_3(BTC)_2$ MOF, because it is one of the prototypical MOFs, its crystals have been grown well on 2-D surfaces,[4,6b,16] and it has demonstrated a wide range of applications such as catalyst[20] and drug delivery.[21] The particles were alternatingly immersed in an ethanol solution of $Cu(OAc)_2$ (0.01 M) and benzene-1,3,5-tricarboxylic acid (H_3BTC, 0.01 M) for 1 min, separated by centrifugation (2000 rpm, 5 min). It was found that two acetate ligands of the paddle wheel $[Cu_2(CH_3COO)_4(H_2O)_2]$ unit in solution of copper acetate are readily displaced by free carboxylate units of the surface and BTC, facilitating the layer-by-layer $Cu_3(BTC)_2$ crystal growth.[22] Between every deposition step, the particles were washed with EtOH and DMF, and isolated by centrifugation. Compared to two-dimensional substrates, very little is known about the reliable growth of MOF's on particles by a layer-by-layer approach, which, in parts, can be attributed to the technical difficulties associated with the separation of the nano- or microparticles during the sequence of multiple growth steps. To date, the only reported example takes advantage of a magnetic separation step.[23] While magnetic separation can result in effective MOF growth, it drastically limits the choice of particles that can be modified by MOF decoration. In order to overcome this obstacle, we evaluated a range of different separation methods and ultimately found centrifugation to be the most applicable separation methods. Every growth cycle was thus comprised of a sequence of 9 steps: 1) Immersion with metal salt, 2) Centrifugation, 3) Washing, 5) Centrifugation, 6) Immersion with ligand, 7) Centrifugation, 8) Washing, 9) Centrifugation (see Supporting Information). The repetition of this layer-by-layer approach altered the colour of bicompartmental particles to become blue. Seven growth cycles were sufficient to cover the seed particles with anisotropically grown MOF nanocrystals (**Figure 4**a-c). The SEM images confirm unambiguously a crystallization boundary between the particle compartments, indicating not only a well-defined compartmentalization due the electrohydrodynamic co-jetting process, but also the successful maintenance of the anisotropic architecture throughout the entire sequence of subsequent processing steps including shape shifting, cross-linking, deprotection, and MOF growth. Finally, the characteristic bands in the powder X-ray diffraction (PXRD) of these particles finally reveal that $Cu_3(BTC)_2$ crystals were successfully grown on the particle hemisphere, affording a new type of organic-inorganic hybrid particles, although the PXRD pattern is greatly dominated by the amorphous nature of the organic polymer matrix, giving rise to a very broad signal at $2\theta \approx 20°$ (Figure 4d).[6c]

To evaluate the potential of multifunctional particles, we went on to create magnetic, MOF-patterned Janus colloids. The selective inclusion of magnetite nanoparticles in a P(*n*BuMA-*co*-CEMA) solution during the co-jetting process provided magnetically and compositionally anisotropic particles. Then, the previously established series of particle modification steps from shape evolution to MOF growth was employed to prepare new hierarchically functionalized composite colloids, as depicted in Figure 4e. The SEM and energy-dispersive X-ray spectroscopy

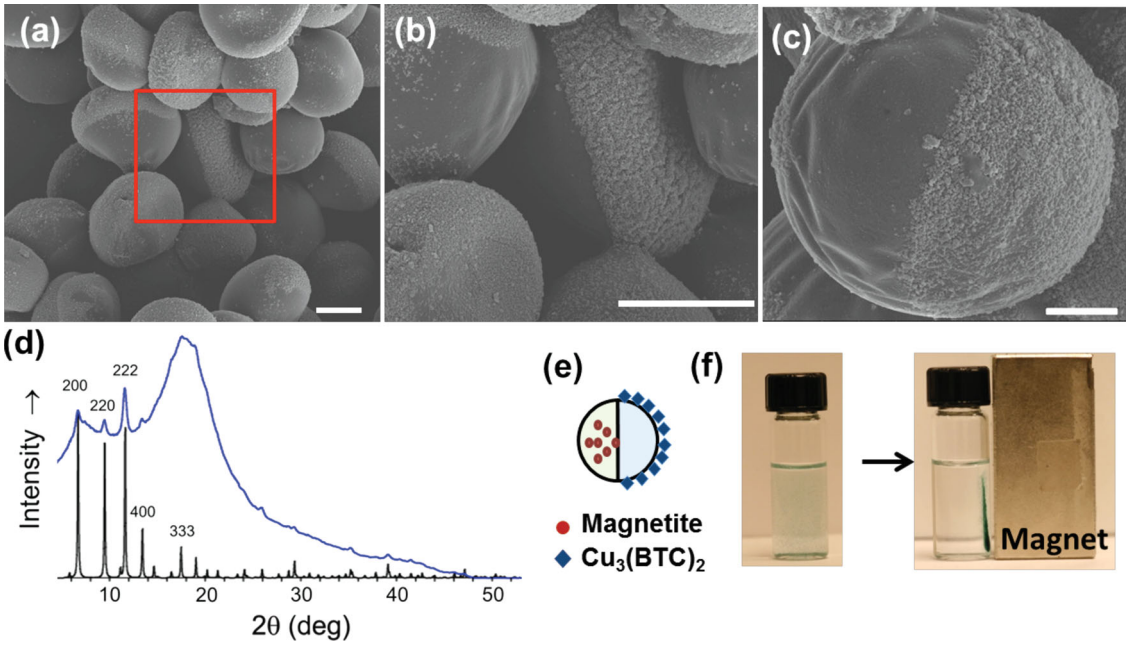

Figure 4. (a)-(c) SEM images of anisotropic $Cu_3(BTC)_2$ nanocrystal-functionalized bicompartmental particles; (b) shows an expanded image of the red square in image (a); scale bar 5 μm (a and b), 2 μm (c). (d) PXRD pattern of MOF-functionalized bicompartmental particles (blue); the black pattern was simulated from the crystal structure of $Cu_3(BTC)_2$. (e) Cartoon of a particle where one compartment embeds magentite and the surface of the opposite one is covered with $Cu_3(BTC)_2$ nanocrystals. (f) Response of magnetite/MOF-functionalized bicompartmental particles to the external magnetic field.

study of particles displays that one hemisphere surface is functionalized with porous MOF nanocrystals and the other hemisphere embraces paramagnetic nanoparticles (Figure S6). Figure 4f demonstrates the response of magnetite/MOF-functionalized bicompartmental particles to the external magnetic field. Initially, the particles were suspended in water. The placement of a magnet on the right side of the vial localized these particles near the magnet, implying capability to magnetically manipulate the hybrid Janus particles.

In summary, we have successfully fabricated spatio-selectively MOF-patched bicompartmental particles via electrohydrodynamic co-jetting, shape evolution, photo-crosslinking, and selective chemical modification and crystallization. Furthermore, the inclusion of paramagnetic nanoparticles into one compartment presented a new kind of hierarchically functionalized organic inorganic hybrid on which porous MOF nanocrystals are magnetically controllable. We, thus, anticipate that these hybrid Janus particles may find applications such as switchable catalysts, delivery vehicles, or smart adsorbents resulting from magnetically controllable porosity.

Supporting Information

Supporting Information is available from the Wiley Online Library or from the author.

Acknowledgements

We acknowledge funding from the Multidisciplinary University Research Initiative of the Department of Defense and the Army Research Office (W911NF-10–1–0518). We also thank the Helmholtz Association for support through the BIF program.

Received: November 3, 2013
Revised: December 4, 2013
Published online: February 14, 2014

[1] a) L. Ma, C. Abney, Wenbin Lin, *Chem. Soc. Rev.* **2009**, *38*, 1248; b) M. Yoon, R. Srirambalaji, K. Kim, *Chem . Rev.* **2012**, *112*, 1196.
[2] J. R. Li, R. J. Kuppler, H.-C. Zhou, *Chem. Soc. Rev.* **2009**, *38*, 1477.
[3] P. Horcajada, R. Gref, T. Baati, P. K. Allan, G. Maurin, P. Couvreur, G. Férey, R. E. Morris, C. Serre, *Chem. Rev.* **2012**, *112*, 1232.
[4] a) O. Shekhah, J. Liu, R. A. Fischer, Ch. Wöll, *Chem. Soc. Rev.* **2011**, *40*, 1081; b) A. Bétard, R. A. Fischer, *Chem. Rev.* **2012**, *112*, 1055; c) P. Falcaro, D. Buso, A. J. Hill, C. M. Doherty, *Adv. Mater.* **2012**, *24*, 3153.
[5] a) R. Ameloot, E. Gobechiya, H. Uji-i, J. A. Martens, J. Hofkens, L. Alaerts, B. F. Sels, D. E. De Vos, *Adv. Mater.* **2010**, *22*, 2685; b) C. M. Doherty, G. Grenci, R. Riccò, J. I. Mardel, J. Reboul, S. Furukawa, S. Kitagawa, A. J. Hill, P. Falcaro, *Adv. Mater.* **2013**, *25*, 4701.
[6] a) H. J. Lee, W. Cho, M. Oh, *Chem. Commun.* **2012**, *48*, 221; b) R. Ameloot, A. Liekens, L. Alaerts, M. Maes, A. Galarneau, B. Coq, G. Desmet, B. F. Sels, J. F. M. Denayer, D. E. De Vos, *Eur. J. Inorg. Chem.* **2010**, 3735.
[7] A. B. Pawar, I. Kretzschmar, *Macromol. Rapid Commun.* **2010**, *31*, 150.
[8] a) S. Crossley, J. Faria, M. Shen, D. E. Resasco, *Science* **2010**, *327*, 68; b) S. Cobo, J. Heidkamp, P.-A. Jacques, J. Fize, V. Fourmond, L. Guetaz, B. Jousselme, V. Ivanova, H. Dau, S. Palacin, M. Fontecave, V. Artero, *Nat . Mater.* **2012**, *11*, 802.
[9] K. J. Lee, J. Yoon, S. Rahmani, S. Hwang, S. Bhaskar, S. Mitragotri, J. Lahann, *Proc. Natl. Acad. Sci.* **2012**, *109*, 16057.

[10] a) J. A. Champion, Y. K. Katare, S. Mitragotri, *Proc. Natl. Acad Sci.* **2007**, *104*, 11901; b) S. Hwang, J. Lahann, *Macromol. Rapid Commun.* **2012**, *33*, 1178.
[11] a) S. H. Kim, J. Y. Sim, J. M. Lim, S. M. Yang, *Angew. Chem. Int. Ed.* **2010**, *49*, 3786; b) S. Hwang, K. H. Roh, D. W. Lim, G. Y. Wang, C. Uher, J. Lahann, *Phys. Chem. Chem. Phys.* **2010**, *12*, 11894.
[12] a) J. Yoon, K. J. Lee, J. Lahann, *J. Mater. Chem.* **2011**, *21*, 8502; b) K. J. Lee, J. Yoon, J. Lahann, *Curr. Opin. Colloid Interface Sci.* **2011**, *16*, 195; c) Q. Chen, S. C. Bae, S. Granick, *Nature* **2011**, *469*, 381; d) *Janus particle synthesis, self-assembly and applications*, (Eds: S. Jiang, S. Granick) , The Royal Society of Chemistry, **2012**
[13] a) J. Lahann, *Small* **2011**, *7*, 1149; b) T.-H. Park, Lahann, in *Janus particle synthesis, self-assembly and applications*, (Eds. S. Jiang, S. Granick) , The Royal Society of Chemistry **2012**, pp. 54–73.
[14] a) K.-H. Roh, D. C. Martin, J. Lahann, *Nat. Mater.* **2005**, *4*, 759; b) J. Lahann, *J. Am. Chem. Soc.* **2009**, *131*, 6650; c) S. Bhaskar, J. Hitt, S.-W.L. Chang, J. Lahann, *Angew. Chem. Int. Ed.* **2009**, *48*, 4589.
[15] a) S. Bhaskar, K. H. Roh, X. W. Jiang, G. L. Baker, J. Lahann, *Macromol. Rapid Commun.* **2008**, *29*, 1655; b) M. Yoshida, K. H. Roh, S. Mandal, S. Bhaskar, D. W. Lim, H. Nandivada, X. P. Deng, J. Lahann, *Adv. Mater.* **2009**, *21*, 4920; c) S. Bhaskar, K. M. Pollock, M. Yoshida, J. Lahann, *Small* **2010**, *6*, 404; d) S. Bhaskar, C. T. Gibson, M. Yoshida, H. Nandivada, X. P. Deng, N. H. Voelcker, J. Lahann, *Small* **2011**, *7*, 812; e) S. Saha, D. Copic, S. Bhaskar, N. Clay, A. Donini, A. J. Hart, J. Lahann, *Angew. Chem. Int. Ed.* **2012**, *51*, 660; f) W. Lv, K. J. Lee, J. Li, T.-H. Park, S. Hwang, A. J. Hart, F. Zhang, J. Lahann, *Small* **2012**, *8*, 3116; g) J. Yoon, A. Kota, S. Bhaskar, A. Tuteja, J. Lahann, *ACS Appl. Mater. Interfaces* **2013**, *5*, 11281
[16] a) S. Hermes, F. Schröder, R. Chelmowski, C. Wöll, R. A. Fischer, *J. Am. Chem. Soc.* **2005**, *127*, 13744; b) O. Shekhah, H. Wang, S. Kowarik, F. Schreiber, M. Paulus, M. Tolan, C. Sternemann, F. Evers, D. Zacher, R. A. Fischer, C. Wöll, *J. Am. Chem. Soc.* **2007**, *129*, 15118.
[17] K. J. Lee, S. Hwang, J. Yoon, S. Bhaskar, T.-H. Park, J. Lahann, *Macromol. Rapid Commun.* **2011**, *32*, 431.
[18] Due to the irregular shape and dimples of as-jetted particles, we determined particle size from SEM images obtained after shape-shifting into sphere and the mean diameter was estimated to be 10 ± 1.3 μm.
[19] S. Mitragotri, J. Lahann, *Nat. Mater.* **2009**, *8*, 15.
[20] A. Sachse, R. Ameloot, B. Coq, F. Fajula, B. Coasne, D. De Vos, A. Galarneau, *Chem. Commun.* **2012**, *48*, 4749.
[21] A. Carné-Sánchez, I. Imaz, M. Cano-Sarabia, D. Maspoch, *Nat. Chem* . **2013**, *5*, 203.
[22] O. Shekhah, H. Wang, D. Zacher, R. A. Fischer, Ch. Wöll, *Angew. Chem. Int. Ed.* **2009**, *48*, 5038.
[23] M.E. Silvestre, M. Franzreb, P.G. Weidler, O. Shekhah, Ch. Wöll, *Adv. Funct. Mater.* **2013**, *23*, 1093.